

1 **Title: Immune chromatin reader SP140 regulates microbiota and risk for inflammatory**
2 **bowel disease**

3 **Authors:**

4 Isabella Fraschilla^{1,2,3}, Hajera Amatullah^{1,2}, Raza-Ur Rahman^{1,2}, Kate L. Jeffrey^{1,2,3}

5
6
7 ¹Division of Gastroenterology and Center for the Study of Inflammatory Bowel Disease,
8 Department of Medicine, Massachusetts General Hospital, Boston, Massachusetts 02114, USA
9

10 ²Harvard Medical School, Boston, Massachusetts 02115, USA
11

12 ³Program in Immunology, Harvard Medical School, Boston, Massachusetts 02115, USA
13 *Correspondence to: KJeffrey@mgh.harvard.edu

14
15 **Abstract:**

16 Inflammatory bowel disease (IBD) is driven by host genetics and environmental factors,
17 including commensal microorganisms. Epigenetics facilitate integration of environmental
18 cues for transcriptional output. However, evidence of epigenetic dysregulation directly
19 causing host-commensal dysbiosis and IBD is lacking. Speckled Protein 140 (SP140) is an
20 immune-restricted chromatin ‘reader’ with homology to Autoimmune Regulator (AIRE).
21 SP140 mutations associate with three immune diseases: Crohn’s disease (CD), multiple
22 sclerosis (MS) and chronic lymphocytic leukemia (CLL), but disease-causing mechanisms
23 remain undefined. Here we identify a critical immune-intrinsic role for SP140 in preventing
24 expansion of inflammatory Proteobacteria, including *Helicobacter* in mice and
25 *Enterobacteriaceae* in humans. Mice harboring altered microbiota due to hematopoietic
26 SP140 deficiency exhibited severe colitis which was transmissible upon co-housing and
27 ameliorated with antibiotics. SP140 was critical for calibration of macrophage microbicidal
28 responses required for normal host-commensal crosstalk and elimination of invasive
29 pathogens. Mutations within this epigenetic reader may constitute a predisposing event in
30 human diseases provoked by the microbiome, such as IBD and MS.
31

32
33 **Introduction**

34 Complex immune diseases, including inflammatory bowel disease (IBD) and multiple
35 sclerosis (MS) are multifactorial diseases that develop as a result of gene-environment
36 interactions (Graham and Xavier, 2020). Genome-wide association studies have identified over
37 240 genetic risk alleles that are associated with the two types of IBD: Ulcerative Colitis (UC) and
38 Crohn’s disease (CD) (Jostins et al., 2012; Liu et al., 2015; Rivas et al., 2011). Many of these risk
39 alleles overlap with loci that associate with MS (International Multiple Sclerosis Genetics et al.,
40 2013) suggesting common disease initiating mechanisms. One shared CD and MS risk allele is
41 SP140. SP140 is an immune-restricted member of the Speckled Protein (SP) epigenetic ‘reader’
42 family, consisting of SP100, SP110, SP140 and SP140L, which have high sequence homology
43 with Autoimmune Regulator (AIRE) (Fraschilla and Jeffrey, 2020). Epigenetic readers are diverse
44 proteins with specialized docking domains that ‘read’ covalent modifications primarily on histones
45 to regulate transcription (Arrowsmith et al., 2012). To achieve this function, SPs all contain 3
46 ‘reader’ domains: 1) a SAND domain (named after the few SAND domain-containing proteins:
47 SP100, AIRE, NucP41/P75, and DEAF) that interacts with DNA directly or through protein-protein
48 interactions, 2) a plant homeodomain (PHD) that docks to histone methylation, and 3) a
49 bromodomain that binds acetylated histones (Bienz, 2006; Bottomley et al., 2001; Filippakopoulos
50 et al., 2012; Waterfield et al., 2014). Although, the PHD of SP140 may be atypical by facilitating
51

52 SUMOylation of the bromodomain and associating with SETDB1, a histone methyltransferase of
53 H3K9 that promotes gene silencing (Garcia-Dominguez et al., 2008; Ivanov et al., 2007; Peng
54 and Wysocka, 2008; Zhang et al., 2016; Zucchelli et al., 2019). In addition, SP140 contains a
55 caspase activation and recruitment domain (CARD) involved in multimerization and co-
56 localization to 'speckled' promyelocytic leukemia (PML) nuclear bodies, macromolecular
57 multiprotein complexes with diverse functionality including transcriptional repression (Corpet et
58 al., 2020; Hoischen et al., 2018; Huoh et al., 2020).

59 Consistent with the predicted role for SP140 in gene silencing, in human macrophages,
60 SP140 was found to predominantly occupy and maintain inaccessibility of promoters of
61 developmentally silenced loci, such as the HOXA cluster (Mehta et al., 2017). HOXA9 is a known
62 promoter of stem-like state in hematopoietic stem cells (HSCs) and an inhibitor of macrophage
63 differentiation and glycolysis (Argiropoulos and Humphries, 2007; Huang et al., 2012;
64 Thorsteinsdottir et al., 2002; Zhou et al., 2018). HOXA9 is therefore normally silenced in mature
65 macrophages (De Santa et al., 2007), but not in SP140-deficient mouse or human macrophages,
66 that ultimately display defective transcriptional responses to bacteria or viral ligands (Mehta et al.,
67 2017). A global proteomics analysis subsequently found that SP140 directly represses
68 topoisomerases to maintain heterochromatin, gene silencing, and macrophage responsiveness
69 (Amatullah et al., 2021). Furthermore, an array of studies has now implicated SP140 as an
70 essential factor in antibacterial, antiviral, and antiparasitic responses (Ji et al., 2021; Madani et
71 al., 2002; Matsushita et al., 2021; Regad and Chelbi-Alix, 2001). However, despite some progress
72 in understanding the function of this enigmatic epigenetic reader in macrophages, the role of
73 SP140 in the immune response to intestinal microbiota, and how disruption of this function due to
74 human genetic variation in SP140 may drive development of Crohn's disease or MS remains
75 unclear.

76 Development of complex immune disorders, such as IBD and MS, is dependent on both
77 host genetics as well as cues derived from intestinal microbes and their metabolites (Amatullah
78 and Jeffrey, 2020; Blander et al., 2017; Graham and Xavier, 2020; Iliev and Cadwell, 2021; Kaiko
79 et al., 2016; Schulthess et al., 2019; Vinolo et al., 2011; Wu et al., 2020). Innate immune pathways
80 are crucial for integrating bacterial, viral and fungal signals from the intestinal microenvironment
81 to regulate gene expression, microbial balance and intestinal homeostasis (Adiliaghdam et al.,
82 2021; Iliev and Cadwell, 2021; Schulthess et al., 2019). Moreover, many IBD-associated
83 mutations are within genes essential for innate immune defense pathways, emphasizing their
84 requirement for maintaining homeostatic host-microorganism relationships (Graham and Xavier,
85 2020; Jostins et al., 2012; Kugelberg, 2014). CD-associated mutations in SP140 result in
86 defective mRNA splicing and a reduction in SP140 protein (Matesanz et al., 2015; Mehta et al.,
87 2017) rendering innate immune cells hypo-responsive. Further, mouse models support that
88 SP140 is normally required for intestinal homeostasis via an innate immune function, as
89 hematopoietic knockdown (Mehta et al., 2017) or whole mouse deletion of Sp140 exacerbates
90 dextran sulfate sodium (DSS)-induced colitis in a manner dependent on macrophages (Amatullah
91 et al., 2021). In this study, we investigated the possible link between intestinal microbial
92 communities and SP140 control of intestinal homeostasis. We found that disruptions in SP140
93 result in a defective microbicidal transcriptome in phagocytes but enhanced activation of CD8+ T
94 cells in colonic lamina propria and colitis. Remarkably, these intestinal malfunctions were
95 dependent on the expansion of Proteobacteria, including *Helicobacter*, that was transmissible
96 upon co-housing with wild-type mice and treated with antibiotics. This was further corroborated in
97 CD patients bearing SP140 loss-of-function mutations that displayed significant elevation in
98 Proteobacteria *Enterobacteriaceae*. Taken together, we have identified a key innate immune-
99 intrinsic role for epigenetic reader SP140 in preventing intestinal inflammation by restricting the
100 pathological expansion of a common member of the intestinal microbiota.

101
102 **Results and discussion**

103 **SP140 is essential for antibacterial pathways in mice and human**

104 SP140 is an essential host regulator of antibacterial defense to *Mycobacterium*
105 *tuberculosis* (*Mtb*) (Ji et al., 2021; Pan et al., 2005; Pichugin et al., 2009) and gram negative
106 bacteria (*Salmonella enterica* serovar *Typhimurium*, *Escherichia coli*, and *Citrobacter rodentium*)
107 (Amatullah et al., 2021). Therefore, we sought to understand the mechanism by which SP140
108 contributes to antibacterial host defense and how SP140 deficiency may impact intestinal
109 microbial dysbiosis and inflammation in CD patients bearing loss-of-function mutations. We
110 examined transcriptional programs of human peripheral blood mononuclear cells (PBMCs)
111 obtained from healthy controls expressing wild-type SP140 (HC SP140^{wt}), Crohn's disease (CD)
112 patients expressing wildtype SP140 (CD SP140^{wt}), or CD patients that were homozygous for CD-
113 associated SP140 mutations (CD SP140^{mut}), obtained through the Prospective Registry
114 in IBD Study at MGH (PRISM) cohort. A prominent gene set downregulated in CD SP140^{mut} cells
115 compared to both healthy controls and CD SP140^{wt} PBMCs included genes associated with
116 bacterial defense (**Fig. 1A**). CD SP140^{mut} cells had reduced expression of transcripts encoding
117 for subunits of NADPH oxidase (*CYBB*, *NCF1*, *NCF2*, *NCF4*) and H⁺-ATPase (*ATP6V0A1*,
118 *ATP6V0D1*), which are known complexes that act at the phagosome to produce antibacterial
119 reactive oxygen species (ROS) and low pH, respectively. Moreover, at steady state, genes
120 essential for the degradation or killing of bacteria, including calprotectin subunits (*S100A8*,
121 *S100A9*), lysozyme (*LYZ*), and cathepsins (*CTSB*, *CTSH*), were also reduced in CD SP140^{mut}
122 cells. Since calprotectin is a well-studied antimicrobial protein capable of enhancing bacterial
123 killing, we confirmed reduced protein levels of calprotectin component S100A8 in CD SP140^{mut}
124 PBMCs compared to SP140^{wt} CD patient donors (**Fig. 1B**).

125 Human and mouse SP140 are only 54% homologous at the amino acid level, owing to
126 inclusion of an intrinsically disorder region (IDR) in human SP140 (Fraschilla and Jeffrey, 2020).
127 However, we found that antimicrobial transcripts, such as *S100a8*, *Lyz2* and *Lcn2*, were also
128 downregulated in *Sp140*^{-/-} bone-marrow derived macrophages (BMDMs) (**Fig. 1C**). The
129 conserved role of SP140 in controlling antimicrobial gene programs suggests that this chromatin
130 reader plays an essential role in host defense. Since previous analysis of genome-wide
131 occupancy of SP140 in human macrophages found that SP140 did not directly occupy
132 antimicrobial gene loci and promoted gene repression at silenced chromatin regions (Mehta et
133 al., 2017), SP140 likely promotes an antibacterial gene program via maintenance of
134 heterochromatin and macrophage identity.

135 SP140 expression has been shown to be immune-restricted and particularly high in
136 macrophages (Mehta et al., 2017). Intestinal macrophages, which differentiate from circulating
137 monocytes (Bain et al., 2014), and other phagocytes in the intestine are responsible for
138 bactericidal responses, namely production of ROS and antimicrobial proteins (Schulthess et al.,
139 2019; Smythies et al., 2005). Furthermore, other IBD-associated loci have similarly been shown
140 to regulate microbial responses in the intestine via epithelial cells (Conway et al., 2013; Graham
141 and Xavier, 2020; Ramanan et al., 2014), which are resistant to irradiation. To determine whether
142 SP140 expression in immune cells is sufficient to protect against intestinal inflammation, we
143 irradiated wildtype (WT) mice and reconstituted them with WT or *Sp140*^{-/-} bone marrow. Mice with
144 specific *Sp140* deficiency in the hematopoietic compartment displayed significantly exacerbated
145 DSS-colitis compared to WT controls, as determined by weight loss (**Fig. 1D**) and colon length
146 (**Fig. 1E**). Thus, *Sp140* within the immune compartment is essential for intestinal homeostasis.
147 To extend our *ex vivo* characterization of antibacterial programs in mouse and human primary
148 cells, we next investigated whether *Sp140* deficiency alters the development of intestinal
149 phagocyte populations that are necessary for bacterial clearance. We performed
150 immunophenotyping of colonic lamina propria CD45⁺ cells by flow cytometry analysis in *Sp140*^{-/-}
151 and WT mice. *Sp140* deficiency did not affect the proportions of mononuclear phagocyte
152 populations (**Fig. S1C**) or B cells (**Fig. S1A, B**) suggesting that recruitment and development of
153 these cell types is intact in *Sp140*^{-/-} mice. However, a dysfunctional response to the microbiota

154 can lead to adaptive immune cell infiltration in the gut (Feng et al., 2010). Indeed, we observed a
155 significant and specific expansion of total CD8⁺ T cells (**Fig. 1F, G**) as well as a significant increase
156 in the frequency and number of activated CD8⁺CD44⁺ T cells (**Fig. 1H, I**) in the colonic lamina
157 propria of *Sp140*^{-/-} mice. Intriguingly, this defect was specific to CD8⁺ T cells as CD4⁺ T cells and
158 CD4⁺CD44⁺ T cell frequencies and numbers were unaltered with *Sp140* deficiency (**Fig. 1F-I**).
159 Taken together, these results show that *Sp140* is required for macrophage antibacterial
160 responses and this defect leads to CD8⁺ T cell activation in the gut lamina propria prior to the
161 manifestation of disease.

162

163 **Cohousing wild-type mice with *Sp140*^{-/-} mice increased severity of induced colitis**

164 Mice with an shRNA-mediated hematopoietic knockdown of *Sp140* and *Sp140*^{-/-} mice
165 generated by CRISPR/Cas9 targeting are more susceptible to DSS-mediated colitis, in a manner
166 dependent on *Sp140* control of cytokine production and bacterial killing in macrophages
167 (Amatullah et al., 2021; Mehta et al., 2017). Further, an abundance of studies has demonstrated
168 that mice deficient in innate immune system components, or cytokines, have altered microbiota
169 with increased inflammatory capacity (Caruso et al., 2019; Elinav et al., 2011; Frederic et al.,
170 2012; Ramanan et al., 2014; Zenewicz et al., 2013). Moreover, presence of activated CD8⁺ T cells
171 in the colon is frequently the result of microbiota dysbiosis (Ramanan et al., 2014; Tanoue et al.,
172 2019; Yu et al., 2020). We therefore questioned whether the microbiota of *Sp140*^{-/-} mice could
173 contribute to the exacerbated colitis phenotype. We designed an experiment in which WT mice
174 were cohoused with *Sp140*^{-/-} mice or were housed separately. After 4 weeks of cohousing, a
175 period previously established to be sufficient for the transmission of microbiota between mice via
176 coprophagia (Stappenbeck and Virgin, 2016; Zenewicz et al., 2013), we administered DSS and
177 examined the resulting weight loss and inflammation associated with colitis. Whereas *Sp140*^{-/-}
178 mice exhibit exacerbated colitis compared to WT mice when housed separately, cohousing WT
179 mice with *Sp140*^{-/-} mice led to enhanced weight loss of WT mice, similar to separated or cohoused
180 *Sp140*^{-/-} mice (**Fig. 2A, B**). To examine inflammation, we measured colon lengths at day 12 post-
181 DSS administration and found significantly shorter colons in WT mice that were cohoused with
182 the *Sp140*^{-/-} mice than WT mice that were housed separately (**Fig. 2C**). Histological examination
183 of colons confirmed an increase in inflammation in WT mice specifically upon co-housing as
184 shown by crypt elongation, thickening of the mucosa, and a leukocyte infiltrate to the level of the
185 lamina submucosa (**Fig. 2D**). The transmission of the altered gut microbiota from *Sp140*^{-/-} mice
186 to cohoused WT mice, along with increased susceptibility to DSS-induced colitis, indicates that
187 the altered gut microbiota works as a contributing factor for, rather than a consequence of, the
188 disease. To understand whether the microbiome of *Sp140*^{-/-} mice is colitogenic due to increased
189 inflammatory capacity, we collected and filtered stool homogenates from untreated *Sp140*^{-/-} mice
190 and controls and stimulated BMDMs *in vitro*. Stool homogenates obtained from *Sp140*^{-/-} mice
191 proved to be hyperinflammatory compared to WT stool, as shown by a significant increase in the
192 production of the pro-inflammatory cytokine Interleukin (IL)-6 (**Fig. 2E**).

193

194 ***Sp140*^{-/-} mice have altered commensal microbiota that is transmissible**

195 Our data support the hypothesis that *Sp140*^{-/-} mice have an altered microbiota that is
196 transmissible to wild-type mice. Thus, we undertook bacterial 16S rRNA gene pyrosequencing to
197 examine the microbiome in four groups of mice: WT mice, *Sp140*^{-/-} mice, and WT mice or *Sp140*^{-/-}
198 mice cohoused with each other. Prior to DSS treatment we collected fecal samples from each
199 mouse, prepared fecal DNA, and used barcoded pyrosequencing of the 16S rRNA gene V4 region
200 to explore the change in the microbiome. A significant increase in community richness in *Sp140*^{-/-}
201 mice was observed. Furthermore, this increase in richness was transferred to cohoused WT
202 mice compared to non-cohoused WT controls (**Fig. 3A**). UniFrac-based principal component
203 analysis (PCA) determined that WT and *Sp140*^{-/-} microbiome communities were significantly

204 dissimilar from each other (**Fig. 3B**). Moreover, this difference was lost upon cohousing whereby
205 WT microbiomes now overlapped with *Sp140^{-/-}* communities, demonstrating a dominance of
206 *Sp140^{-/-}* microbiota (**Fig. 3B**). Proportional taxonomy analysis revealed that *Sp140^{-/-}* mouse stool
207 contained a higher percentage of Proteobacteria phyla than WT mice, and Proteobacteria then
208 bloomed in WT cohoused mice (**Fig. 3C**) thus identifying a putative, transmissible bacteria of the
209 *Sp140^{-/-}* mouse microbiome that may confer sensitivity to colitis. Proteobacteria expansion is
210 associated with worsened colitis in mouse models (Garrett et al., 2010; Ni et al., 2017).
211 Furthermore, we specifically determined that *Sp140^{-/-}* intestines were colonized by a greater
212 percentage of classes *Epsilonproteobacteria* and *Alphaproteobacteria* (**Fig. 3D**). Conversely,
213 *Sp140^{-/-}* exhibited reduced Verrucomicrobia phyla that are present in wild-type controls (**Fig. 3C**).
214 Unbiased Linear discriminant analysis Effect Size (LEfSe) analysis determined a significant
215 elevation of colitis-driving *Helicobacter* genera of the *Epsilonproteobacteria* class and
216 *Mucispirillum* genera of the *Deferribacteria* phylum in *Sp140^{-/-}* mice compared to WT controls (**Fig.**
217 **3E**). Notably, a significant reduction in the protective *Akkermansia muciniphila* was also observed
218 in *Sp140^{-/-}* mice (**Fig. 3E**). Furthermore, the *Sp140* deficient microbiome was efficiently transferred
219 to cohoused WT mice (**Fig. 3F**) to the point where no significant differences were detected
220 between *Sp140^{-/-}* mice and WT cohoused mice by LEfSe analysis (**Fig. 3G-H**). Thus, *Sp140*
221 deficiency triggers the development of a colitogenic microbiome, that is efficiently transferred
222 upon cohousing.

223 The *Helicobacter* genus can drive colitis and inflammation in mice (Cahill et al., 1997; Chai
224 et al., 2017; Kullberg et al., 1998; Yang et al., 2013) while *A. muciniphila* promotes mucosal wound
225 healing and ameliorates colitis in mouse models (Alam et al., 2016; Ansaldi et al., 2019). We
226 therefore confirmed the significant elevation in *Helicobacter* and reduction in *A. muciniphila* in
227 *Sp140^{-/-}* feces by qPCR (**Fig. 3I**). To assess if *Sp140* control of microbiota was intrinsic to innate
228 immune cells, or if there was a role for lymphocytes, we crossed *Sp140^{-/-}* mice with lymphocyte-
229 deficient *Rag1^{-/-}* mice and found that feces from double mutant *Sp140^{-/-}Rag1^{-/-}* mice still displayed
230 significantly elevated *Helicobacter* and reduced *A. muciniphila* (**Fig. 3J**). Thus, *Sp140* deficiency
231 specifically in innate cells drives proteobacteria expansion. Furthermore, this data demonstrates
232 that the elevation in activated CD8⁺ T cells in the colonic lamina propria of *Sp140^{-/-}* mice (**Fig. 1F-**
233 **I**) is indeed a consequence of microbiota disruption.

234

235 Crohn's disease patients with *SP140* mutations exhibit increase in intestinal 236 *Enterobacteriaceae*

237 Our analysis of intestinal bacterial populations in *Sp140^{-/-}* mice suggest that a bloom of
238 pathogenic Proteobacteria results in exacerbated colitis. To demonstrate that expanded
239 Proteobacteria was a driving factor of exacerbated colitis in *Sp140^{-/-}* mice, we administered mice
240 the antibiotic metronidazole via drinking water for 2 weeks before DSS-colitis induction. Indeed,
241 metronidazole treatment protected *Sp140^{-/-}* mice from inflammation associated with colitis as
242 determined by increased colon length (**Fig. 4A**) and reduced crypt hyperplasia (**Fig. 4B**)
243 compared to *Sp140^{-/-}* mice that did not receive antibiotics. Metronidazole targets gram-negative
244 anaerobes, including species within the Proteobacteria phylum, and is used in the clinic to treat
245 CD. In order to determine whether manipulation of the microbiota might be a beneficial route of
246 treatment in CD patients bearing *SP140* loss-of-function mutations, we sought to determine
247 whether the architecture of microbial communities in *Sp140^{-/-}* mice recapitulated species
248 dominance in humans with *SP140* loss-of-function. We performed 16S sequencing analysis of
249 stool obtained from healthy controls, CD *SP140^{wt}*, and CD *SP140^{mut}* individuals (**Fig. S2A**). Alpha-
250 diversity analysis determined that stool from CD patients exhibited reduced Shannon diversity
251 compared to healthy controls (**Fig. 4C**) as previously reported (Franzosa et al., 2019). However,
252 each group segregated from each other in principal component analysis (**Fig. 4D**) demonstrating
253 that while both CD *SP140^{wt}* and CD *SP140^{mut}* individuals lose bacterial diversity, there are
254 compositional differences between these two groups of CD patients. Proportional taxonomy

255 analysis demonstrated that Proteobacteria diversity was lost in CD SP140^{mut} individuals whereby
256 Gammaproteobacteria dominates (**Fig. 4E**). Specifically, we observed a significant increase in
257 *Enterobacteriaceae*, a family of Gammaproteobacteria, in CD patients bearing SP140 loss-of-
258 function mutations (**Fig. 4F**). The *Enterobacteriaceae* family of the Proteobacteria phylum
259 encompasses gram negative facultative anaerobes including *Escherichia coli*, *Citrobacter*
260 *rodentium*, and *Salmonella enterica*. Blooming of facultative anaerobes, particularly
261 *Enterobacteriaceae*, with a concomitant depletion of obligate anaerobes associated with short
262 chain fatty acid production is a common feature of IBD gut microbiomes (Knights et al., 2014;
263 Lloyd-Price et al., 2019; Morgan et al., 2012). Furthermore, *Enterobacteriaceae* blooms are
264 associated with chronic inflammation and treatment failure in IBD (Olbjørn et al., 2019; Walujkar
265 et al., 2014). We predict that the inability to initiate production of toxic reactive oxygen species
266 and antibacterial proteins in SP140-deficient CD patients permits expansion of
267 *Enterobacteriaceae* as has been suggested for individuals with loss-of-function mutations in
268 NAPDH oxidase subunits (Denson et al., 2018; Muise et al., 2012; Plichta et al., 2019).

269 IBD symptoms and severity are a spectrum, suggesting that subtypes of disease are
270 dependent on an axis of genetics, environmental cues, and epigenetics. Understanding how risk
271 alleles contribute to pathogenicity and how epigenetic dysregulation is a contributing factor to IBD
272 is essential for identifying disease subtypes as well as developing precision medicine treatment
273 options. Here we have identified a key regulatory role for a novel epigenetic reader protein,
274 SP140, that is also a risk allele for IBD, in the maintenance of macrophage function and prevention
275 of intestinal microbe expansion, specifically Proteobacteria members. These findings have
276 important implications for not only CD patients with loss-of-function SP140 mutations but also for
277 MS that is driven by an altered microbiota. Genetic loss of SP140 has drastic consequences on
278 the composition of the microbial communities leading to a shift towards a pro-inflammatory
279 configuration that could predispose, and contribute to phenotypes of, both CD and MS (Berer et
280 al., 2011) (Berer et al., 2017; Britton et al., 2019; Britton et al., 2020; Cekanaviciute et al., 2017),
281 as well as other diseases influenced by genetics and microbe-derived factors. These results shed
282 light on the etiology of CD and provide insight into the relationship between genetic susceptibility,
283 epigenetics, microbial dysbiosis and the immune response in the gut. Patients with SP140
284 mutations may benefit from targeting pro-inflammatory commensals through targeted antibiotics
285 or fecal transplants.

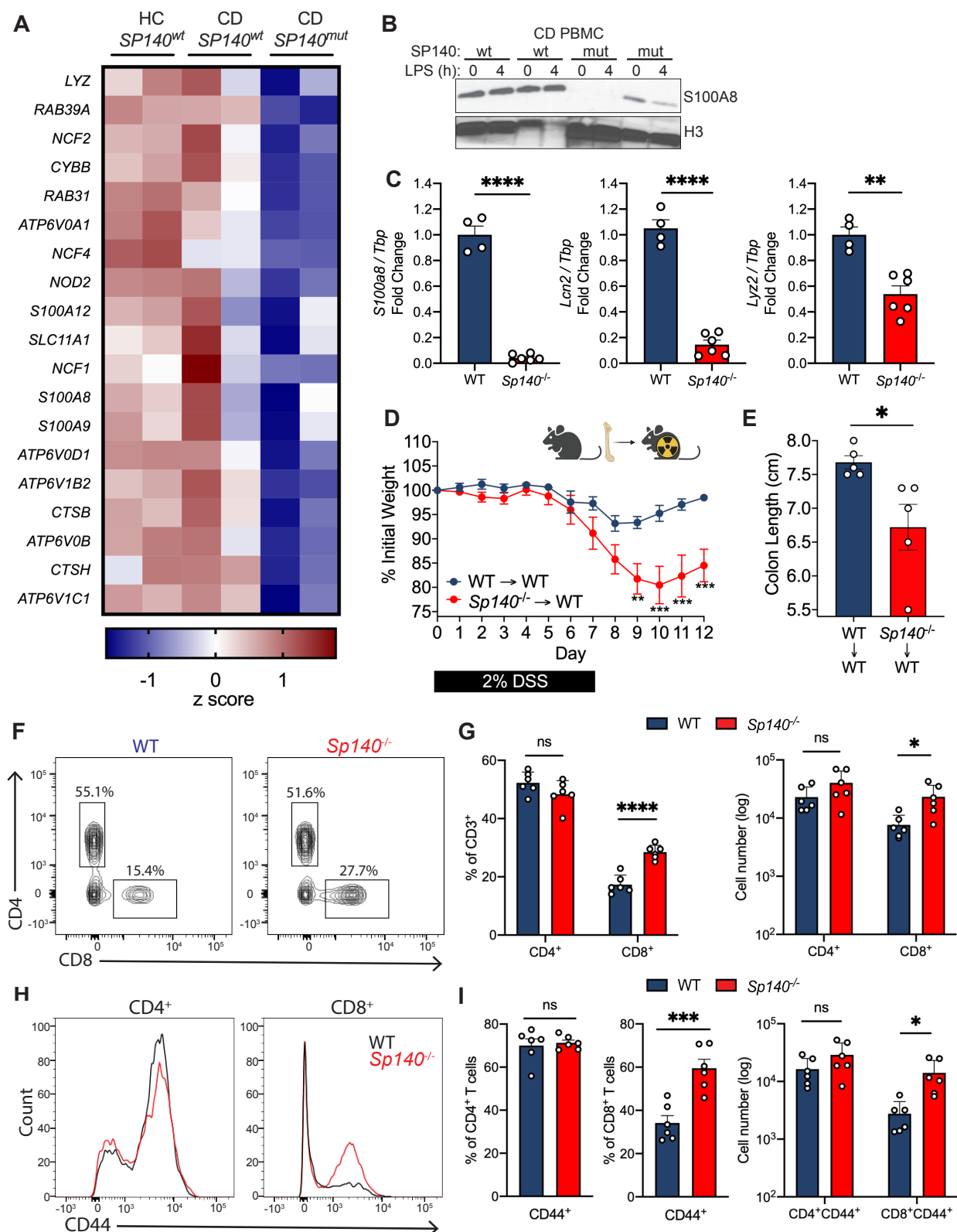


Figure 1. SP140 is essential for antimicrobial gene programs in mouse and human. (A) Heat map of genes down-regulated ($\log_2\text{FC} > 2$) in human peripheral blood mononuclear cells (PBMC)

from healthy controls (HC), Crohn's disease (CD) patients bearing wildtype *SP140* (*SP140*^{wt}) or CD-risk *SP140* genetic variant (*SP140*^{mut}) (n=2, RNA-seq) from [GSE89876](#). **(B)** Immunoblot of S100A8 in PBMC from *SP140*^{wt} or *SP140*^{mut} CD patients after 0 or 4 hours LPS stimulation (100 ng/mL). **(C)** Expression of mouse *S100a8*, *Lcn2*, and *Lyz2* mRNA relative to *Tbp*, as determined by qPCR, in mouse bone marrow-derived macrophages (BMDMs) from wildtype (WT) and *Sp140*^{-/-} mice. **(D)** Daily body weight of WT and *Sp140*^{-/-} mice and **(E)** quantification of day 12 colon lengths after 2% dextran sodium sulfate (DSS) administration (n=5). **(F-I)** Flow cytometry analysis of WT and *Sp140*^{-/-} mouse colon lamina propria (n=6). **(F)** Representative flow cytometry plots of live CD45⁺CD3⁺ cells gated on CD4⁺ and CD8⁺ T cells. **(G)** Quantification of frequency and total count of CD4⁺ and CD8⁺ T cells. **(H)** Representative histogram overlay of CD44 expression in CD4⁺ and CD8⁺ T cells. **(I)** Quantification of frequency and total count of CD44⁺CD4⁺ and CD8⁺ T cells. Data are mean of 2-6 biological replicates. *P<0.05, **P<0.01, ***P< 0.001, ****P<0.0001; unpaired t tests for (C), (E), (F), (H), two-way ANOVA for (D). Error bars represent s.e.m.

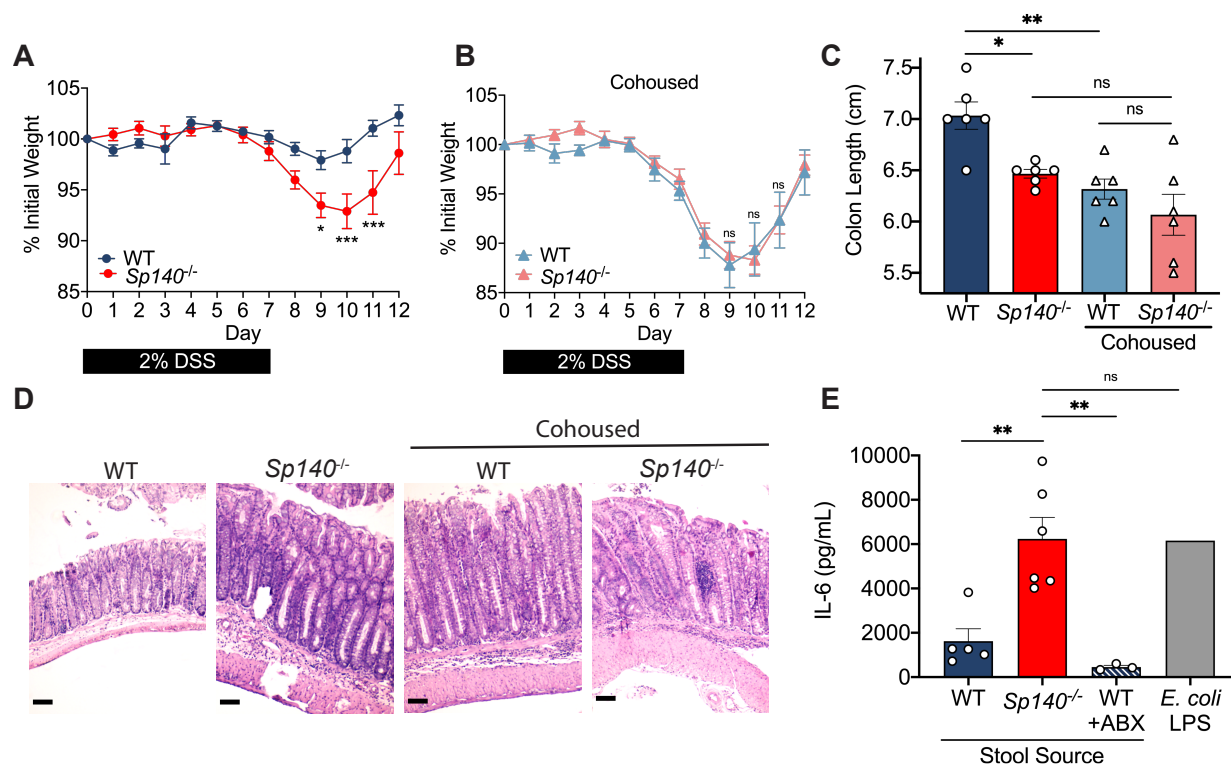


Figure 2. The pro-inflammatory intestinal microbiome of *Sp140*^{-/-} mice is transferable and exacerbates colitis. **(A)** Daily body weight of separately housed wildtype (WT) and *Sp140*^{-/-} mice after 2% dextran sodium sulfate (DSS) administration (n=6). **(B)** Daily body weight of cohoused WT and *Sp140*^{-/-} mice after 2% dextran sodium sulfate (DSS) administration (n=6). **(C)** Day 12 colon lengths of separated or cohoused WT and *Sp140*^{-/-} mice after 2% DSS administration (n=6). **(D)** Representative hematoxylin and eosin-stained sections of day 12 distal colon tissue from separated or cohoused WT and *Sp140*^{-/-} mice after 2% DSS administration. **(E)** IL-6 production, as determined by ELISA, of bone marrow-derived macrophages (BMDMs) supernatants after 16 hours stimulation with LPS (1mg/mL) or stool homogenates (1mg/mL) from WT (n=5), *Sp140*^{-/-} (n=6), or broad-spectrum antibiotic treated WT mice (n=3); representative of 3 experiments. *P < 0.05, **P < 0.01, ***P < 0.001, ****P<0.0001, two-way ANOVA for (A) and (B), one-way ANOVA for (C) and (E). Error bars represent s.e.m.

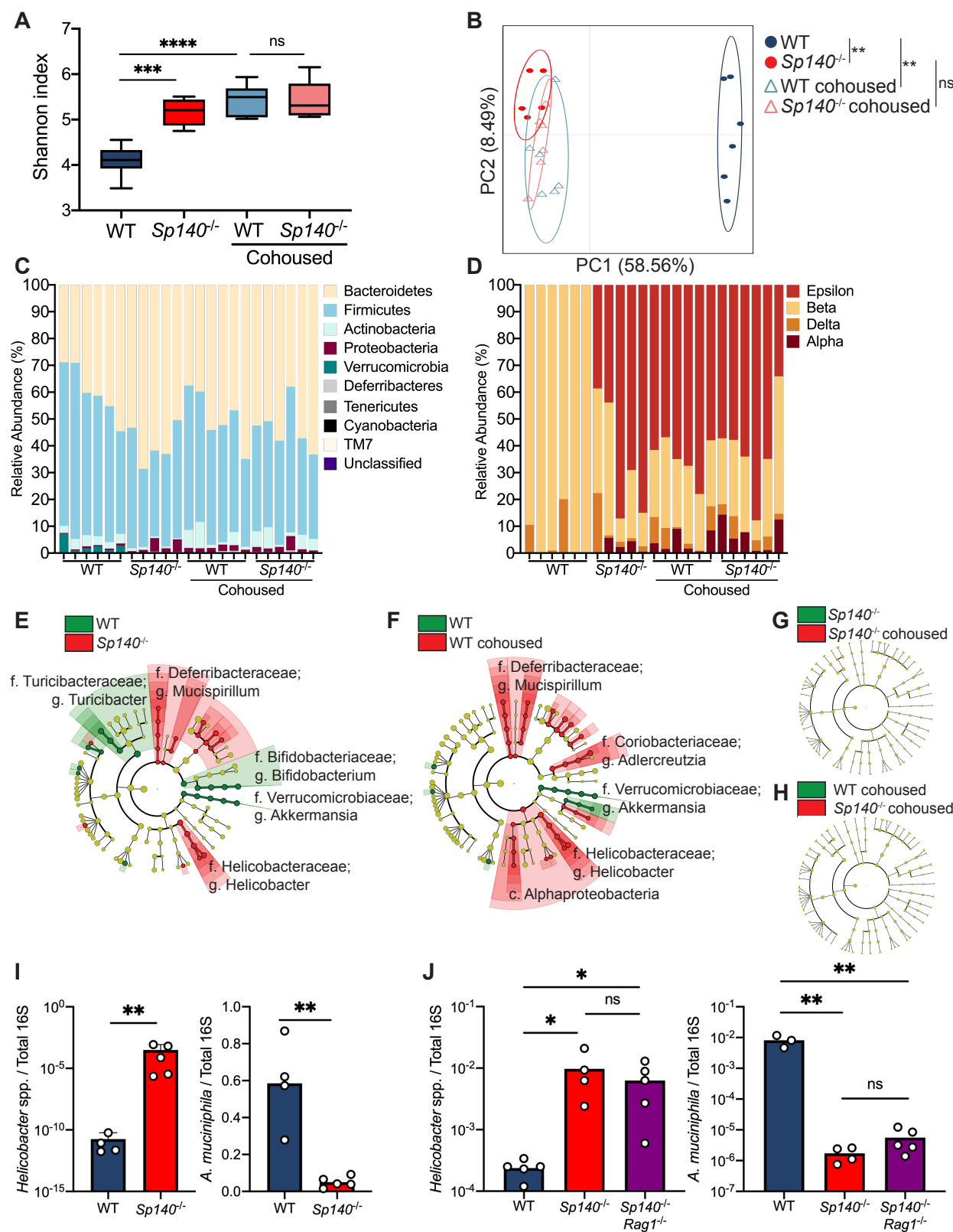


Figure 3. Sp140 deficiency in mice permits a *Helicobacter* bloom and a reduction in *Akkermansia*. (A) Diversity of fecal bacterial communities of separately housed or cohoused wildtype (WT) and *Sp140*^{-/-} mice as determined by Shannon Index. (B) Principal Coordinate

Analysis (PCA), $P<0.05$, PERMANOVA on unweighted UniFrac distance. **(C)** Distribution of bacterial phyla operational taxonomic units presented as relative abundance in each sample. **(D)** Distribution of bacterial class operational taxonomic units presented as relative abundance of Proteobacteria in each sample. **(E)** The compositional differences between separately housed WT and $Sp140^{-/-}$ mice, **(F)** separately housed WT and WT cohoused with $Sp140^{-/-}$ mice, **(G)** separately house $Sp140^{-/-}$ and cohoused $Sp140^{-/-}$ mice, and **(H)** cohoused WT and $Sp140^{-/-}$ mice were determined by a linear discriminant analysis using LEfSe (<https://huttenhower.sph.harvard.edu/galaxy/>). **(I)** Expression of *Helicobacter* species (spp.) and *Akkermansia muciniphila* 16S rRNA relative to total 16S rRNA, as determined by qPCR, in stool from WT and $Sp140^{-/-}$ mice ($n=4-5$). **(J)** Expression of *Helicobacter* species (spp.) and *Akkermansia muciniphila* 16S rRNA relative to total 16S rRNA in stool from WT, $Sp140^{-/-}$, and $Sp140^{-/-}Rag1^{-/-}$ mice ($n=3-5$). * $P < 0.05$, ** $P < 0.01$, *** $P < 0.001$, **** $P < 0.0001$. Error bars represent s.e.m. **(I)** unpaired *t* tests. **(A, J)** one-way ANOVA. * $P < 0.05$, ** $P < 0.01$, *** $P < 0.001$, **** $P < 0.0001$. Error bars represent s.e.m.

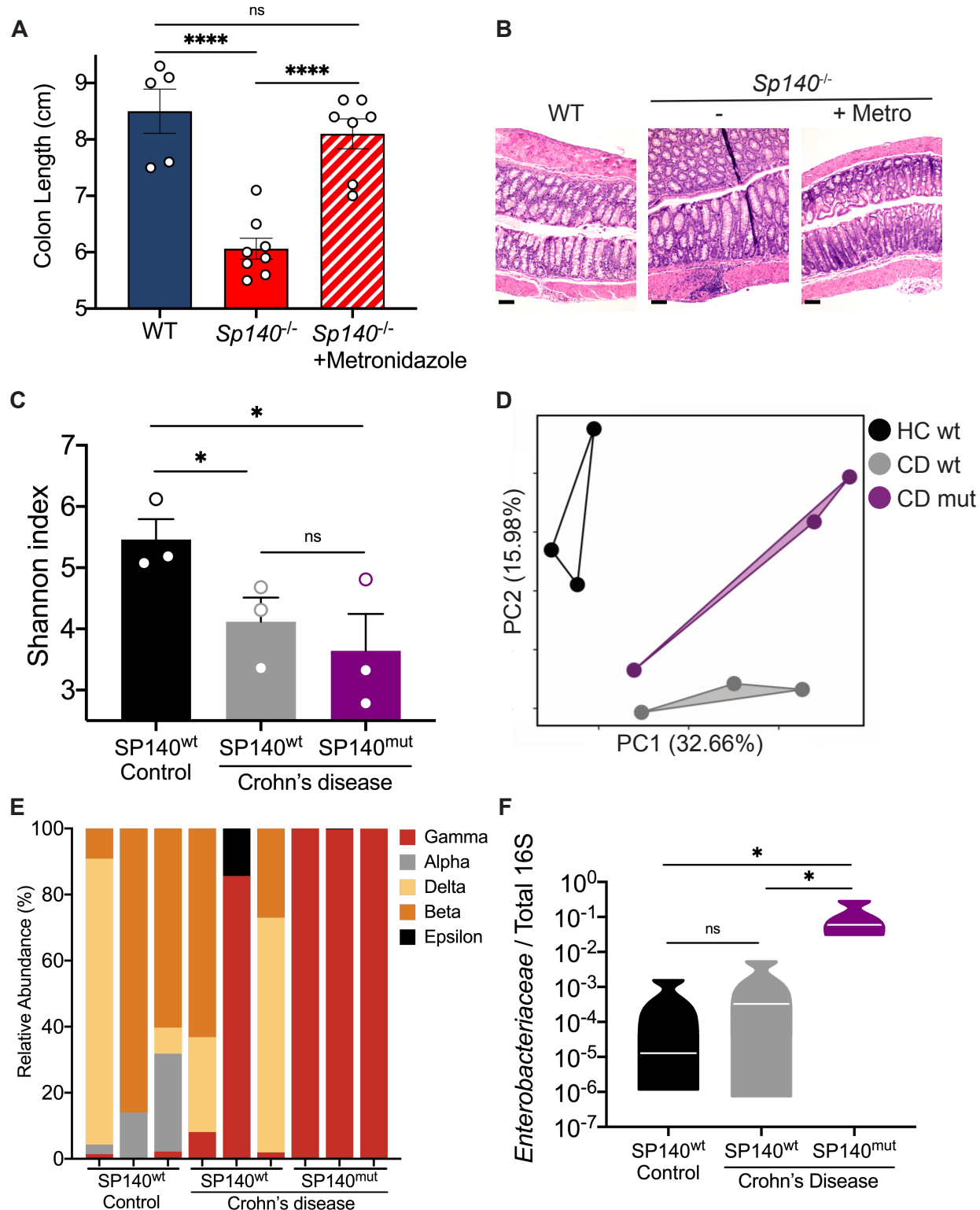


Figure 4. CD-associated *SP140* loss-of-function variant associates with increased intestinal *Enterobacteriaceae* in humans. (A) Day 12 colon lengths of WT, *Sp140*^{-/-}, and *Sp140*^{-/-} mice treated with or without metronidazole and administered 2% dextran sodium sulfate (DSS).

(B) Representative hematoxylin and eosin-stained sections of day 12 distal colon tissue after 2% DSS administration to WT, *Sp140*^{-/-}, and *Sp140*^{-/-} mice treated with metronidazole (metro). **(C)** Diversity of fecal bacterial communities of healthy controls, Crohn's disease (CD) patients expressing wildtype SP140 (SP140^{WT}), and CD patients bearing the common SP140 genetic variant (SP140^{MUT}). **(D)** Principal Coordinate Analysis (PCA), P<0.05, PERMANOVA on unweighted UniFrac distance. **(E)** Distribution of bacterial class operational taxonomic units presented as relative abundance of Proteobacteria in each sample. **(F)** Expression of *Enterobacteriaceae* 16S rRNA relative to total 16S rRNA in human stool. (A-B) n=5-8; (C-F) n=3, one-way ANOVA. *P < 0.05, **P < 0.01, ***P < 0.001, ****P<0.0001. Error bars represent s.e.m.

Author Contributions

I.F. performed and interpreted *in vitro* and *in vivo* experiments, with help from H.A. R-U.R performed analysis of 16S sequencing. K.L.J conceived and supervised the study, acquired funding and wrote the final manuscript, along with I.F.

Acknowledgements

We sincerely thank the clinical coordinators and patients enrolled in the Prospective Registry in IBD study at Massachusetts General Hospital (PRISM), Russell Vance (University of California, Berkeley) for *Sp140*^{-/-} mice, Amy Avery (Massachusetts General Hospital) for technical assistance with 16S sequencing, the entire Jeffrey lab for valuable scientific discussions as well as Robert Anthony, James Moon, Charles Evavold, and Jonathan Kagan for critical reading of the manuscript. This study was supported by F31DK127518 (I.F.), the Kenneth Rainin Foundation (Innovator and Synergy Awards to K.L.J), NIH R01DK119996 (K.L.J), K.L.J is a John Lawrence MGH Research Scholar 2020-2025.

Competing interests. K.L.J. is an employee of Moderna Inc., 200 Technology Square, Cambridge MA 02138, since November 2021. K.L.J is a member of the scientific advisory board for Ancilia Biosciences. None of these relationships influenced with work in this study.

Materials and Methods

Mice

C57BL/6J mice were originally purchased from Jackson Laboratory and bred in-house. All mice were bred and housed under specific pathogen-free conditions according to the National Institutes of Health (NIH). All animal experiments were conducted under protocols approved by the MGH Institutional Animal Care and Use Committee (IACUC), and in compliance and appropriate ethical regulations. For all experiments, age- and sex-matched mice were used. *Sp140*^{-/-} mice were made on C57BL/6J background as previously characterized (Ji et al., 2021). *Rag1*^{-/-} mice were purchased from Jackson Laboratory and crossed to *Sp140*^{-/-} mice. For cohousing experiments, WT and *Sp140*^{-/-} mice were cohoused from weaning for 4 weeks at a 2:2 ratio per cage.

Human blood and stool samples

All human samples were collected under Institutional Review Board (IRB)-approved protocols by Massachusetts General Hospital (MGH), including informed consent obtained in accordance with relevant ethical regulations. Blood and stool samples were collected from patients that were enrolled in the "Prospective Registry in IBD Study at Massachusetts General Hospital (PRISM, IRB# FWA00003136). Study research coordinators obtained consent, and medical history was obtained and confirmed by review of the electronic medical record. Human peripheral blood mononuclear cells (PBMCs) were obtained from healthy human volunteers (Blood Components Lab, Massachusetts General Hospital) or from Crohn's disease patients from the Prospective Registry in IBD study at Massachusetts General Hospital (PRISM) genotyped by CD-risk SP140 SNPs rs28445040 and rs6716753. Patient metadata is provided in **Figure S2**. Briefly,

mononuclear cells were isolated by density gradient centrifugation of PBS-diluted buffy coat/blood (1:2) over Ficoll-Paque Plus (GE Healthcare). The PBMC layer was carefully removed and washed 3 times with PBS.

Western blot

For Immunoblotting of PBMCs or human macrophages, 2.5 million cells were used and cell lysates were prepared by incubation and sonication of cells in RIPA buffer (10 mM Tris-Cl (pH 8.0), 1 mM EDTA, 0.5 mM EGTA, 1% Triton X-100, 0.1% sodium deoxycholate, 0.1% SDS, 140 mM NaCl). 20 µg protein was electrophoresed per lane on NuPAGE Novex Bis-Tris 4–12% Gels (Invitrogen) and transferred to PVDF membranes using iBlot dry blotting system (Invitrogen). The following antibodies were used: anti-S100A8 (Abcam; ab92331), anti-H3 (Abcam; ab18521).

Quantitative PCR

RNA was extracted from cells using the RNeasy Mini Kit (Qiagen) with on-column DNase digest (Qiagen) according to manufacturer's instructions. cDNA was synthesized from isolated RNA by reverse transcription using the iScript cDNA Synthesis Kit (Bio-Rad) according to the manufacturer's instructions. In the case of quantitative PCR performed on stool DNA, QIAamp DNA Stool Mini Kit was used to extract DNA from feces. Quantitative PCR was performed using iTaq Universal SYBR Green Supermix (Bio-Rad) according to the manufacturer's instructions. To analyze relative mRNA levels, derived values were normalized to indicated housekeeping genes. qPCR primers were purchased from Sigma-Aldrich. A complete list of primer sequences is provided in Supplementary Table 1.

Bone marrow-derived macrophages

Bone marrow-derived macrophages (BMDMs) were produced from WT or Sp140-deficient mice. Bone marrow was flushed from tibia and femur and allowed to adhere to a non-treated tissue culture plate for 1 day. Non-adherent cells were then differentiated to macrophages in DMEM containing 10% FBS, 1% L-Glutamine, 1% penicillin/streptomycin, 0.1% β -mercaptoethanol, 5ng/mL of interleukin 3 (IL-3, Peprotech) and macrophage colony stimulating factor (M-CSF, Peprotech) for 7 days. Macrophage maturity was assessed by surface expression of CD11b and F4/80 with flow cytometry.

Flow cytometry

For flow cytometric analysis, colons were dissected, and caeca were removed. The tissue was placed in RPMI containing 5% FBS and fat was removed by careful dissection followed by gentle rolling along a moist paper towel. The tissue was cut open longitudinally and rinsed to remove loose fat and fecal matter. Colon was cut into 1-2 cm pieces and transferred to RPMI containing 5% FBS, 5mM EDTA, and 1mM DTT and incubated at 37C for 20 minutes with shaking (400rpm). To remove epithelial cells, colons were next vigorously shaken in complete RPMI with 2mM EDTA. Colon was minced into fine pieces and digested in complete RPMI containing 0.5 mg/mL Dispase II (Gibco) and 1.5 mg/mL type IV collagenase (Gibco) for 45 minutes at 37C shaking (400rpm). Single-cell suspensions were prepared using a 40um nylon cell strainer. Cells were stained with fixable live/dead stain, Fc Block, counting beads, and fluorochrome-conjugated antibodies for 20 min on ice then fixed on ice for 30 min using Fixation/Permeabilization Solution Kit. Data were acquired using a BD FACSAria running FACSDiva software and analyzed with FlowJo software. Mononuclear phagocytes were analyzed using a previously described gating strategy (Adiliaghdam et al., 2021). See Supplemental Table 2 for a list of FACS antibodies and reagents used.

Mouse bone marrow reconstitution

Bone marrow progenitor cells obtained from C57BL/6 donor mice were placed in 24-well tissue culture dishes (1×10^6 cells per well) in fresh media containing 15% fetal bovine serum, IL-3 (20 ng/ml), IL-6 (50 ng/ml), and stem cell factor (SCF) (50 ng/ml). On day 4, the cells were harvested and washed twice in PBS. For bone marrow transplantation, C57BL/6 recipient mice were irradiated with 131Cs at 10 gray on day 0 and injected retro-orbitally with 2.5×10^6 bone marrow cells in 200 μ l of Dulbecco's modified Eagle's medium, after which the mice were monitored for 6 weeks to allow for immune reconstitution.

Dextran sodium sulfate (DSS)-colitis

Mice were administered 2% dextran sodium sulfate salt (DSS, MW = 36,000-50,000 Da; MP Biomedicals) in drinking water ad libitum for 7 days (freshly prepared every other day), followed by regular drinking water for 5 days. Mice were sacrificed on day 12. Colon length was measured. For histology, tissue was collected from the distal part of the colon, and hematoxylin and eosin staining were performed. Images were obtained on an EVOS XL Core Imaging System microscope (ThermoFisher). Metronizadole treated mice were administered 1g/L metronidazole drinking water with 8mg/mL Sweet'N Low for 2 weeks prior to the start of DSS administration and continued through day 12.

16S rRNA gene sequencing

QIAamp DNA Stool Mini Kit was used to extract DNA from mouse and human feces. The hypervariable region (V4) of the 16S rRNA gene sequences were amplified by using PCR with adaptor primer set containing 12bp multiplex identifier sequences (Integrated DNA Technologies, Coralville, IA). Each reaction contained template DNA, each primer (0.2 μ M), and 2 \times PlatinumTM Hot Start PCR Master Mix (Invitrogen, Carlsbad, CA). PCR conditions were as follows: 94°C for 3 min, followed by 22 cycles at 94°C for 45 sec, 52°C for 1 min, and 72°C for 1.5 min and a final extension step at 72°C for 10 min. Triplicate reactions were prepared, pooled, and purified using SpeedBeadTM carboxylate magnetic bead solution (GE Healthcare, Marlborough, MA). The amplicons were quantified using KAPA Library Quantitation kit (KAPA, Cape Town, South Africa) and an equimolar amount of each sample was sequenced on the MiSeq System (Illumina, San Diego, CA) with 2 \times 150 paired-end run parameters. Microbiome bioinformatics analysis was performed with QIIME 2 release 2018.11. In brief, cutadapt was used to trim 515F/806R primers in the paired end sequences. Subsequently, the sequences were stripped of noise by using the DADA2 denoiser program. The denoised, trimmed and higher quality amplicon sequence variants (ASVs) were aligned with MAFFT and used to construct a phylogeny with fasttree2. All ASVs were assigned taxonomy using the q2-feature-classifier. In brief, a naïve Bayes classifier was trained on the Greengenes 13_8 99% OTUs reference sequences to assign taxonomy to each ASV. The compositional differences among the groups were determined by a linear discriminant analysis using LEfSe (Segata et al., 2011) with a threshold of 2.0 on the logarithmic score and alpha value of 0.01 for the factorial Kruskal-Wallis test among classes using Galaxy (<https://huttenhower.sph.harvard.edu/galaxy/>). 16S rRNA sequencing data are deposited at Sequencing Read Archive (SRA) under accession number SAMN26873569.

Macrophage stimulations with stool homogenates

Stool pellets were weighed and resuspended in 40mg/mL complete DMEM then homogenized using a BeadBug 3 microtube homogenizer (Benchmark Scientific) for 9 minutes at highest speed in BeadBug tubes containing 1.5mm Zirconium beads. Homogenized stool was centrifuged at 400g for 1 min. Supernatant was collected and passed through 70 μ m strainer. Stool homogenates were then added to 0.5×10^6 bone marrow-derived macrophages (BMDMs) in a 96 well plate at a final concentration of 1mg/mL. Antibiotic treated mice were administered a broad-spectrum antibiotic cocktail (1g/L metronidazole, 0.5g/L vancomycin, 1g/L ampicillin, 1g/L neomycin) containing 8mg/mL Sweet'N Low via drinking water. Stool was collected after 4 weeks of antibiotic

treatment. Mouse IL-6 was measured in cell supernatants using a DuoSet ELISA kit per manufacturer instructions (R&D Systems).

Software

Flow cytometry samples were acquired using FACSDiva and analyzed using FlowJo version 10. Statistical analysis was performed using GraphPad Prism version 7.

References

Adiliaghdam, F., H. Amatullah, S. Digumarthi, T.L. Saunders, R.-U. Rahman, L.P. Wong, R. Sadreyev, L. Droit, J. Paquette, P. Goyette, J. Rioux, R. Hodin, K.A. Mihindukulasuriya, S.A. Handley, and K.L. Jeffrey. 2021. Human enteric viruses shape disease phenotype through divergent innate immunomodulation. *bioRxiv*. doi:10.1101/2021.10.14.464404.

Alam, A., G. Leoni, M. Quiros, H. Wu, C. Desai, H. Nishio, R.M. Jones, A. Nusrat, and A.S. Neish. 2016. The microenvironment of injured murine gut elicits a local pro-restitutive microbiota. *Nature Microbiology* 1:15021.

Amatullah, H., S. Digumarthi, I. Fraschilla, F. Adiliaghdam, G. Bonilla, L.P. Wong, R.I. Sadreyev, and K.L. Jeffrey. 2021. Identification of topoisomerase as a precision-medicine target in chromatin reader SP140-driven Crohn's disease. 10.1101/2021.09.20.461083.

Amatullah, H., and K.L. Jeffrey. 2020. Epigenome-metabolome-microbiome axis in health and IBD. *Curr Opin Microbiol* 56:97-108.

Ansaldo, E., L.C. Slayden, K.L. Ching, M.A. Koch, N.K. Wolf, D.R. Plichta, E.M. Brown, D.B. Graham, R.J. Xavier, J.J. Moon, and G.M. Barton. 2019. Akkermansia muciniphila induces intestinal adaptive immune responses during homeostasis. *Science* 364:1179-1184.

Argiropoulos, B., and R.K. Humphries. 2007. Hox genes in hematopoiesis and leukemogenesis. *Oncogene* 26:6766-6776.

Arrowsmith, C.H., C. Bountra, P.V. Fish, K. Lee, and M. Schapira. 2012. Epigenetic protein families: a new frontier for drug discovery. *Nat Rev Drug Discov* 11:384-400.

Bain, C.C., A. Bravo-Blas, C.L. Scott, E. Gomez Perdigero, F. Geissmann, S. Henri, B. Malissen, L.C. Osborne, D. Artis, and A.M. Mowat. 2014. Constant replenishment from circulating monocytes maintains the macrophage pool in the intestine of adult mice. *Nature Immunology* 15:929-937.

Berer, K., L.A. Gerdés, E. Cekanaviciute, X. Jia, L. Xiao, Z. Xia, C. Liu, L. Klotz, U. Stauffer, S.E. Baranzini, T. Kümpfel, R. Hohlfeld, G. Krishnamoorthy, and H. Wekerle. 2017. Gut microbiota from multiple sclerosis patients enables spontaneous autoimmune encephalomyelitis in mice. *Proceedings of the National Academy of Sciences* 114:10719-10724.

Berer, K., M. Mues, M. Koutrolos, Z.A. Rasbi, M. Boziki, C. Johner, H. Wekerle, and G. Krishnamoorthy. 2011. Commensal microbiota and myelin autoantigen cooperate to trigger autoimmune demyelination. *Nature* 479:538-541.

Bienz, M. 2006. The PHD finger, a nuclear protein-interaction domain. *Trends in Biochemical Sciences* 31:35-40.

Blander, J.M., R.S. Longman, I.D. Iliev, G.F. Sonnenberg, and D. Artis. 2017. Regulation of inflammation by microbiota interactions with the host. *Nature Immunology* 18:851-860.

Bottomley, M.J., M.W. Collard, J.I. Huggenvik, Z. Liu, T.J. Gibson, and M. Sattler. 2001. *Nature Structural Biology* 8:626-633.

Britton, G.J., E.J. Conti, I. Mogno, O.H. Vennaro, S.R. Llewellyn, R. Ng, Z. Li, A. Mortha, M. Merad, A. Das, D. Gevers, D.P.B. McGovern, N. Singh, J. Braun, J.P. Jacobs, J.C. Clemente, A. Grinspan, B.E. Sands, J.-F. Colombel, M.C. Dubinsky, and J.J. Faith. 2019. Microbiotas from Humans with Inflammatory Bowel Disease Alter the Balance of Gut Th17 and ROR γ T Cells and Exacerbate Colitis in Mice. *Immunity* 50:212-224.e214.

Britton, G.J., E.J. Contijoch, M.P. Spindler, V. Aggarwala, B. Dogan, G. Bongers, L. San Mateo, A. Baltus, A. Das, D. Gevers, T.J. Borody, N.O. Kaakoush, M.A. Kamm, H. Mitchell, S. Paramsothy, J.C. Clemente, J.F. Colombel, K.W. Simpson, M.C. Dubinsky, A. Grinspan, and J.J. Faith. 2020. Defined microbiota transplant restores Th17/ROR γ mat(+) regulatory T cell balance in mice colonized with inflammatory bowel disease microbiotas. *Proc Natl Acad Sci U S A* 117:21536-21545.

Cahill, R.J., C.J. Foltz, J.G. Fox, C.A. Dangler, F. Powrie, and D.B. Schauer. 1997. Inflammatory bowel disease: an immunity-mediated condition triggered by bacterial infection with *Helicobacter hepaticus*. *Infect Immun* 65:3126-3131.

Caruso, R., T. Mathes, E.C. Martens, N. Kamada, A. Nusrat, N. Inohara, and G. Nunez. 2019. A specific gene-microbe interaction drives the development of Crohn's disease-like colitis in mice. *Sci Immunol*. doi:10.1126/sciimmunol.aaw4341.

Cekanaviciute, E., B.B. Yoo, T.F. Runia, J.W. Debelius, S. Singh, C.A. Nelson, R. Kanner, Y. Bencosme, Y.K. Lee, S.L. Hauser, E. Crabtree-Hartman, I.K. Sand, M. Gacias, Y. Zhu, P. Casaccia, B.A.C. Cree, R. Knight, S.K. Mazmanian, and S.E. Baranzini. 2017. Gut bacteria from multiple sclerosis patients modulate human T cells and exacerbate symptoms in mouse models. *Proceedings of the National Academy of Sciences* 114:10713-10718.

Chai, J.N., Y. Peng, S. Rengarajan, B.D. Solomon, T.L. Ai, Z. Shen, J.S.A. Perry, K.A. Knoop, T. Tanoue, S. Narushima, K. Honda, C.O. Elson, R.D. Newberry, T.S. Stappenbeck, A.L. Kau, D.A. Peterson, J.G. Fox, and C.S. Hsieh. 2017. Helicobacter species are potent drivers of colonic T cell responses in homeostasis and inflammation. *Sci Immunol*. doi:10.1126/sciimmunol.aal5068.

Conway, K.L., P. Kuballa, J.H. Song, K.K. Patel, A.B. Castoreno, O.H. Yilmaz, H.B. Jijon, M. Zhang, L.N. Aldrich, E.J. Villablanca, J.M. Peloquin, G. Goel, I.A. Lee, E. Mizoguchi, H.N. Shi, A.K. Bhan, S.Y. Shaw, S.L. Schreiber, H.W. Virgin, A.F. Shamji, T.S. Stappenbeck, H.C. Reinecker, and R.J. Xavier. 2013. Atg16l1 is Required for Autophagy in Intestinal Epithelial Cells and Protection of Mice From *Salmonella* Infection. *Gastroenterology* 145:1347-1357.

Corpet, A., C. Kleijwegt, S. Roubille, F. Juillard, K. Jacquet, P. Texier, and P. Lomonte. 2020. PML nuclear bodies and chromatin dynamics: catch me if you can! *Nucleic Acids Research* 48:11890-11912.

De Santa, F., M.G. Totaro, E. Prosperini, S. Notarbartolo, G. Testa, and G. Natoli. 2007. The Histone H3 Lysine-27 Demethylase Jmjd3 Links Inflammation to Inhibition of Polycomb-Mediated Gene Silencing. *Cell* 130:1083-1094.

Denson, L.A., I. Jurickova, R. Karns, K.A. Shaw, D.J. Cutler, D.T. Okou, A. Dodd, K. Quinn, K. Mondal, B.J. Aronow, Y. Haberman, A. Linn, A. Price, R. Bezold, K. Lake, K. Jackson, T.D. Walters, A. Griffiths, R.N. Baldassano, J.D. Noe, J.S. Hyams, W.V. Crandall, B.S. Kirschner, M.B. Heyman, S. Snapper, S.L. Guthery, M.C. Dubinsky, N.S. Leleiko, A.R. Otley, R.J. Xavier, C. Stevens, M.J. Daly, M.E. Zwick, and S. Kugathasan. 2018. Clinical and Genomic Correlates of Neutrophil Reactive Oxygen Species Production in Pediatric Patients With Crohn's Disease. *Gastroenterology* 154:2097-2110.

Elinav, E., T. Strowig, Andrew, J. Henao-Mejia, Christoph, Carmen, David, J. Bertin, Stephanie, Jeffrey, and Richard. 2011. NLRP6 Inflammasome Regulates Colonic Microbial Ecology and Risk for Colitis. *Cell* 145:745-757.

Feng, T., L. Wang, T.R. Schoeb, C.O. Elson, and Y. Cong. 2010. Microbiota innate stimulation is a prerequisite for T cell spontaneous proliferation and induction of experimental colitis. *Journal of Experimental Medicine* 207:1321-1332.

Filippakopoulos, P., S. Picaud, M. Mangos, T. Keates, J.P. Lambert, D. Barsyte-Lovejoy, I. Felletar, R. Volkmer, S. Muller, T. Pawson, A.C. Gingras, C.H. Arrowsmith, and S. Knapp.

2012. Histone recognition and large-scale structural analysis of the human bromodomain family. *Cell* 149:214-231.

Franzosa, E.A., A. Sirota-Madi, J. Avila-Pacheco, N. Fornelos, H.J. Haiser, S. Reinker, T. Vatanen, A.B. Hall, H. Mallick, L.J. McIver, J.S. Sauk, R.G. Wilson, B.W. Stevens, J.M. Scott, K. Pierce, A.A. Deik, K. Bullock, F. Imhann, J.A. Porter, A. Zhernakova, J. Fu, R.K. Weersma, C. Wijmenga, C.B. Clish, H. Vlamakis, C. Huttenhower, and R.J. Xavier. 2019. Gut microbiome structure and metabolic activity in inflammatory bowel disease. *Nature Microbiology* 4:293-305.

Fraschilla, I., and K.L. Jeffrey. 2020. The Speckled Protein (SP) Family: Immunity's Chromatin Readers. *Trends in Immunology* 41:572-585.

Frederic, O. Koren, Julia, Malin, I. Nalbantoglu, Jesse, Y. Su, B. Chassaing, William, A. González, Jose, Tyler, N. Barnich, A. Darfeuille-Michaud, M. Vijay-Kumar, R. Knight, Ruth, and Andrew. 2012. Transient Inability to Manage Proteobacteria Promotes Chronic Gut Inflammation in TLR5-Deficient Mice. *Cell Host & Microbe* 12:139-152.

Garcia-Dominguez, M., R. March-Diaz, and J.C. Reyes. 2008. The PHD Domain of Plant PIAS Proteins Mediates Sumoylation of Bromodomain GTE Proteins. *Journal of Biological Chemistry* 283:21469-21477.

Garrett, W.S., C.A. Gallini, T. Yatsunenko, M. Michaud, A. Dubois, M.L. Delaney, S. Punit, M. Karlsson, L. Bry, J.N. Glickman, J.I. Gordon, A.B. Onderdonk, and L.H. Glimcher. 2010. Enterobacteriaceae Act in Concert with the Gut Microbiota to Induce Spontaneous and Maternally Transmitted Colitis. *Cell Host & Microbe* 8:292-300.

Graham, D.B., and R.J. Xavier. 2020. Pathway paradigms revealed from the genetics of inflammatory bowel disease. *Nature* 578:527-539.

Hoischen, C., S. Monajembashi, K. Weisshart, and P. Hemmerich. 2018. Multimodal Light Microscopy Approaches to Reveal Structural and Functional Properties of Promyelocytic Leukemia Nuclear Bodies. *Front Oncol* 8:125.

Huang, Y., K. Sitwala, J. Bronstein, D. Sanders, M. Dandekar, C. Collins, G. Robertson, J. Macdonald, T. Cezard, M. Bilenky, N. Thiessen, Y. Zhao, T. Zeng, M. Hirst, A. Hero, S. Jones, and J.L. Hess. 2012. Identification and characterization of Hoxa9 binding sites in hematopoietic cells. *Blood* 119:388-398.

Huoh, Y.-S., B. Wu, S. Park, D. Yang, K. Bansal, E. Greenwald, W.P. Wong, D. Mathis, and S. Hur. 2020. Dual functions of Aire CARD multimerization in the transcriptional regulation of T cell tolerance. *Nature Communications*. doi:10.1038/s41467-020-15448-w.

Iliev, I.D., and K. Cadwell. 2021. Effects of Intestinal Fungi and Viruses on Immune Responses and Inflammatory Bowel Diseases. *Gastroenterology* 160:1050-1066.

International Multiple Sclerosis Genetics, C., A.H. Beecham, N.A. Patsopoulos, D.K. Xifara, M.F. Davis, A. Kemppinen, C. Cotsapas, T.S. Shah, C. Spencer, D. Booth, A. Goris, A. Oturai, J. Saarela, B. Fontaine, B. Hemmer, C. Martin, F. Zipp, S. D'Alfonso, F. Martinelli-Boneschi, B. Taylor, H.F. Harbo, I. Kockum, J. Hillert, T. Olsson, M. Ban, J.R. Oksenberg, R. Hintzen, L.F. Barcellos, C. Wellcome Trust Case Control, I.B.D.G.C. International, C. Agliardi, L. Alfredsson, M. Alizadeh, C. Anderson, R. Andrews, H.B. Sondergaard, A. Baker, G. Band, S.E. Baranzini, N. Barizzone, J. Barrett, C. Bellenguez, L. Bergamaschi, L. Bernardinelli, A. Berthele, V. Biberacher, T.M. Binder, H. Blackburn, I.L. Bomfim, P. Brambilla, S. Broadley, B. Brochet, L. Brundin, D. Buck, H. Butzkueven, S.J. Caillier, W. Camu, W. Carpentier, P. Cavalla, E.G. Celius, I. Coman, G. Comi, L. Corrado, L. Cosemans, I. Cournu-Rebeix, B.A. Cree, D. Cusi, V. Damotte, G. Defer, S.R. Delgado, P. Deloukas, A. di Sario, A.T. Dilthey, P. Donnelly, B. Dubois, M. Duddy, S. Edkins, I. Elovaara, F. Esposito, N. Evangelou, B. Fiddes, J. Field, A. Franke, C. Freeman, I.Y. Frohlich, D. Galimberti, C. Gieger, P.A. Gourraud, C. Graetz, A. Graham, V. Grummel, C. Guaschino, A. Hadjixenofontos, H. Hakonarson, C. Halfpenny, G. Hall, P. Hall, A. Hamsten, J. Harley, T. Harrower, C. Hawkins, G. Hellenthal, C. Hillier, J. Hobart, M. Hoshi,

S.E. Hunt, M. Jagodic, I. Jelcic, A. Jochim, B. Kendall, A. Kermode, T. Kilpatrick, K. Koivisto, I. Konidari, T. Korn, H. Kronsbein, C. Langford, M. Larsson, M. Lathrop, C. Lebrun-Frenay, J. Lechner-Scott, M.H. Lee, M.A. Leone, V. Leppa, G. Liberatore, B.A. Lie, C.M. Lill, M. Linden, J. Link, F. Luessi, J. Lycke, F. Macciardi, S. Mannisto, C.P. Manrique, R. Martin, V. Martinelli, D. Mason, G. Mazibrada, C. McCabe, I.L. Mero, J. Mescheriakova, L. Moutsianas, K.M. Myhr, G. Nagels, R. Nicholas, P. Nilsson, F. Piehl, M. Pirinen, S.E. Price, H. Quach, M. Reunanan, W. Robberecht, N.P. Robertson, M. Rodegher, D. Rog, M. Salvetti, N.C. Schnetz-Boutaud, F. Sellebjerg, R.C. Selter, C. Schaefer, S. Shaunak, L. Shen, S. Shields, V. Siffrin, M. Slee, P.S. Sorensen, M. Sorosina, M. Sospedra, A. Spurkland, A. Strange, E. Sundqvist, V. Thijs, J. Thorpe, A. Ticca, P. Tienari, C. van Duijn, E.M. Visser, S. Vucic, H. Westerlind, J.S. Wiley, A. Wilkins, J.F. Wilson, J. Winkelmann, J. Zajicek, E. Zindler, J.L. Haines, M.A. Pericak-Vance, A.J. Ivinson, G. Stewart, D. Hafler, S.L. Hauser, A. Compston, G. McVean, P. De Jager, S.J. Sawcer, and J.L. McCauley. 2013. Analysis of immune-related loci identifies 48 new susceptibility variants for multiple sclerosis. *Nat Genet* 45:1353-1360.

Ivanov, A.V., H. Peng, V. Yurchenko, K.L. Yap, D.G. Negorev, D.C. Schultz, E. Psulkowski, W.J. Fredericks, D.E. White, G.G. Maul, M.J. Sadofsky, M.M. Zhou, and F.J. Rauscher, 3rd. 2007. PHD domain-mediated E3 ligase activity directs intramolecular sumoylation of an adjacent bromodomain required for gene silencing. *Mol Cell* 28:823-837.

Ji, D.X., K.C. Witt, D.I. Kotov, S.R. Margolis, A. Louie, V. Chevée, K.J. Chen, M. Gaidt, H.S. Dhaliwal, A.Y. Lee, S.L. Nishimura, D.S. Zamboni, I. Kramnik, D. A. Portnoy, K.H. Darwin, and R.E. Vance. 2021. Role of the transcriptional regulator SP140 in resistance to bacterial infections via repression of type I interferons. *eLife*. doi:10.7554/elife.67290.

Jostins, L., S. Ripke, R.K. Weersma, R.H. Duerr, D.P. McGovern, K.Y. Hui, J.C. Lee, L.P. Schumm, Y. Sharma, C.A. Anderson, J. Essers, M. Mitrovic, K. Ning, I. Cleynen, E. Theatre, S.L. Spain, S. Raychaudhuri, P. Goyette, Z. Wei, C. Abraham, J.P. Achkar, T. Ahmad, L. Amininejad, A.N. Ananthakrishnan, V. Andersen, J.M. Andrews, L. Baidoo, T. Balschun, P.A. Bampton, A. Bitton, G. Boucher, S. Brand, C. Buning, A. Cohain, S. Cichon, M. D'Amato, D. De Jong, K.L. Devaney, M. Dubinsky, C. Edwards, D. Ellinghaus, L.R. Ferguson, D. Franchimont, K. Fransen, R. Gearry, M. Georges, C. Gieger, J. Glas, T. Haritunians, A. Hart, C. Hawkey, M. Hedl, X. Hu, T.H. Karlsen, L. Kupcinskas, S. Kugathasan, A. Latiano, D. Laukens, I.C. Lawrance, C.W. Lees, E. Louis, G. Mahy, J. Mansfield, A.R. Morgan, C. Mowat, W. Newman, O. Palmieri, C.Y. Ponsioen, U. Potocnik, N.J. Prescott, M. Regueiro, J.I. Rotter, R.K. Russell, J.D. Sanderson, M. Sans, J. Satsangi, S. Schreiber, L.A. Simms, J. Sventoraityte, S.R. Targan, K.D. Taylor, M. Tremelling, H.W. Verspaget, M. De Vos, C. Wijmenga, D.C. Wilson, J. Winkelmann, R.J. Xavier, S. Zeissig, B. Zhang, C.K. Zhang, H. Zhao, I.B.D.G.C. International, M.S. Silverberg, V. Annese, H. Hakonarson, S.R. Brant, G. Radford-Smith, C.G. Mathew, J.D. Rioux, E.E. Schadt, M.J. Daly, A. Franke, M. Parkes, S. Vermeire, J.C. Barrett, and J.H. Cho. 2012. Host-microbe interactions have shaped the genetic architecture of inflammatory bowel disease. *Nature* 491:119-124.

Kaiko, G.E., S.H. Ryu, O.I. Koues, P.L. Collins, L. Solnica-Krezel, E.J. Pearce, E.L. Pearce, E.M. Oltz, and T.S. Stappenbeck. 2016. The Colonic Crypt Protects Stem Cells from Microbiota-Derived Metabolites. *Cell* 165:1708-1720.

Knights, D., M.S. Silverberg, R.K. Weersma, D. Gevers, G. Dijkstra, H. Huang, A.D. Tyler, S. van Sommeren, F. Imhann, J.M. Stempak, H. Huang, P. Vangay, G.A. Al-Ghalith, C. Russell, J. Sauk, J. Knight, M.J. Daly, C. Huttenhower, and R.J. Xavier. 2014. Complex host genetics influence the microbiome in inflammatory bowel disease. *Genome Med* 6:107.

Kugelberg, E. 2014. Curbing gut inflammation. *Nature Reviews Immunology* 14:583-583.

Kullberg, M.C., J.M. Ward, P.L. Gorelick, P. Caspar, S. Hieny, A. Cheever, D. Jankovic, and A. Sher. 1998. Helicobacter hepaticus triggers colitis in specific-pathogen-free interleukin-10

(IL-10)-deficient mice through an IL-12- and gamma interferon-dependent mechanism. *Infect Immun* 66:5157-5166.

Liu, J.Z., S. Van Sommeren, H. Huang, S.C. Ng, R. Alberts, A. Takahashi, S. Ripke, J.C. Lee, L. Jostins, T. Shah, S. Abedian, J.H. Cheon, J. Cho, N.E. Daryani, L. Franke, Y. Fuyuno, A. Hart, R.C. Juyal, G. Juyal, W.H. Kim, A.P. Morris, H. Poustchi, W.G. Newman, V. Midha, T.R. Orchard, H. Vahedi, A. Sood, J.J.Y. Sung, R. Malekzadeh, H.-J. Westra, K. Yamazaki, S.-K. Yang, J.C. Barrett, A. Franke, B.Z. Alizadeh, M. Parkes, T. B K, M.J. Daly, M. Kubo, C.A. Anderson, and R.K. Weersma. 2015. Association analyses identify 38 susceptibility loci for inflammatory bowel disease and highlight shared genetic risk across populations. *Nature Genetics* 47:979-986.

Lloyd-Price, J., C. Arze, A.N. Ananthakrishnan, M. Schirmer, J. Avila-Pacheco, T.W. Poon, E. Andrews, N.J. Ajami, K.S. Bonham, C.J. Brislawn, D. Casero, H. Courtney, A. Gonzalez, T.G. Graeber, A.B. Hall, K. Lake, C.J. Landers, H. Mallick, D.R. Plichta, M. Prasad, G. Rahnavard, J. Sauk, D. Shungin, Y. Vázquez-Baeza, R.A. White, J. Braun, L.A. Denson, J.K. Jansson, R. Knight, S. Kugathasan, D.P.B. McGovern, J.F. Petrosino, T.S. Stappenbeck, H.S. Winter, C.B. Clish, E.A. Franzosa, H. Vlamakis, R.J. Xavier, and C. Huttenhower. 2019. Multi-omics of the gut microbial ecosystem in inflammatory bowel diseases. *Nature* 569:655-662.

Madani, N., R. Millette, E.J. Platt, M. Marin, S.L. Kozak, D.B. Bloch, and D. Kabat. 2002. Implication of the Lymphocyte-Specific Nuclear Body Protein Sp140 in an Innate Response to Human Immunodeficiency Virus Type 1. *Journal of Virology* 76:11133-11138.

Matesanz, F., V. Potenciano, M. Fedetz, P. Ramos-Mozo, M. Abad-Grau Mdel, M. Karaky, C. Barriónuevo, G. Izquierdo, J.L. Ruiz-Pena, M.I. Garcia-Sánchez, M. Lucas, O. Fernandez, L. Leyva, D. Otaegui, M. Munoz-Cullia, J. Olascoaga, K. Vandenbroeck, I. Alloza, I. Astobiza, A. Antiguedad, L.M. Villar, J.C. Alvarez-Cermeno, S. Malhotra, M. Comabella, X. Montalban, A. Saiz, Y. Blanco, R. Arroyo, J. Varade, E. Urcelay, and A. Alcina. 2015. A functional variant that affects exon-skipping and protein expression of SP140 as genetic mechanism predisposing to multiple sclerosis. *Hum Mol Genet* 24:5619-5627.

Matsushita, K., X. Li, Y. Nakamura, D. Dong, K. Mukai, M. Tsai, S.B. Montgomery, and S.J. Galli. 2021. The role of Sp140 revealed in IgE and mast cell responses in Collaborative Cross mice. *JCI Insight* 6:2379-3708.

Mehta, S., D.A. Cronkite, M. Basavappa, T.L. Saunders, F. Adiliaghdam, H. Amatullah, S.A. Morrison, J.D. Pagan, R.M. Anthony, P. Tonnerre, G.M. Lauer, J.C. Lee, S. Digumarthi, L. Pantano, S.J. Ho Sui, F. Ji, R. Sadreyev, C. Zhou, A.C. Mullen, V. Kumar, Y. Li, C. Wijmenga, R.J. Xavier, T.K. Means, and K.L. Jeffrey. 2017. Maintenance of macrophage transcriptional programs and intestinal homeostasis by epigenetic reader SP140. *Sci Immunol.* doi:10.1126/sciimmunol.aag3160.

Morgan, X.C., T.L. Tickle, H. Sokol, D. Gevers, K.L. Devaney, D.V. Ward, J.A. Reyes, S.A. Shah, N. LeLeiko, S.B. Snapper, A. Bousvaros, J. Korzenik, B.E. Sands, R.J. Xavier, and C. Huttenhower. 2012. Dysfunction of the intestinal microbiome in inflammatory bowel disease and treatment. *Genome Biol* 13:R79.

Muise, A.M., W. Xu, C.-H. Guo, T.D. Walters, V.M. Wolters, R. Fattouh, G.Y. Lam, P. Hu, R. Murchie, M. Sherlock, J.C. Gana, R.K. Russell, M. Glogauer, R.H. Duerr, J.H. Cho, C.W. Lees, J. Satsangi, D.C. Wilson, A.D. Paterson, A.M. Griffiths, M.S. Silverberg, and J.H. Brumell. 2012. NADPH oxidase complex and IBD candidate gene studies: identification of a rare variant in NCF2 that results in reduced binding to RAC2. *Gut* 61:1028-1035.

Ni, J., T.D. Shen, E.Z. Chen, K. Bittinger, A. Bailey, M. Roggiani, A. Sirota-Madi, E.S. Friedman, L. Chau, A. Lin, I. Nissim, J. Scott, A. Lauder, C. Hoffmann, G. Rivas, L. Albenberg, R.N. Baldassano, J. Braun, R.J. Xavier, C.B. Clish, M. Yudkoff, H. Li, M. Goulian, F.D.

Bushman, J.D. Lewis, and G.D. Wu. 2017. A role for bacterial urease in gut dysbiosis and Crohn's disease. *Sci Transl Med.* doi:10.1126/scitranslmed.aah6888.

Olbjørn, C., M. Cvancarova Småstuen, E. Thiis-Evensen, B. Nakstad, M.H. Vatn, J. Jahnsen, P. Ricanek, S. Vatn, A.E. Moen, T.M. Tannæs, J.C. Lindstrøm, J.D. Söderholm, J. Halfvarson, F. Gomollón, C. Casén, M.K. Karlsson, R. Kalla, A.T. Adams, J. Satsangi, and G. Perminow. 2019. Fecal microbiota profiles in treatment-naïve pediatric inflammatory bowel disease - associations with disease phenotype, treatment, and outcome. *Clinical and Experimental Gastroenterology* Volume 12:37-49.

Pan, H., B.-S. Yan, M. Rojas, Y.V. Shebzukhov, H. Zhou, L. Kobzik, D.E. Higgins, M.J. Daly, B.R. Bloom, and I. Kramnik. 2005. Ipr1 gene mediates innate immunity to tuberculosis. *Nature* 434:767-772.

Peng, J., and J. Wysocka. 2008. It takes a PHD to SUMO. *Trends Biochem Sci* 33:191-194.

Pichugin, A.V., B.S. Yan, A. Sloutsky, L. Kobzik, and I. Kramnik. 2009. Dominant role of the sst1 locus in pathogenesis of necrotizing lung granulomas during chronic tuberculosis infection and reactivation in genetically resistant hosts. *Am J Pathol* 174:2190-2201.

Plichta, D.R., D.B. Graham, S. Subramanian, and R.J. Xavier. 2019. Therapeutic Opportunities in Inflammatory Bowel Disease: Mechanistic Dissection of Host-Microbiome Relationships. *Cell* 178:1041-1056.

Ramanan, D., M.S. Tang, R. Bowcutt, P. Loke, and K. Cadwell. 2014. Bacterial sensor Nod2 prevents inflammation of the small intestine by restricting the expansion of the commensal *Bacteroides vulgatus*. *Immunity* 41:311-324.

Regad, T., and M.K. Chelbi-Alix. 2001. Role and fate of PML nuclear bodies in response to interferon and viral infections. *Oncogene* 20:7274-7286.

Rivas, M.A., M. Beaudoin, A. Gardet, C. Stevens, Y. Sharma, C.K. Zhang, G. Boucher, S. Ripke, D. Ellinghaus, N. Burtt, T. Fennell, A. Kirby, A. Latiano, P. Goyette, T. Green, J. Halfvarson, T. Haritunians, J.M. Korn, F. Kuruvilla, C. Lagacé, B. Neale, K.S. Lo, P. Schumm, L. Törkvist, M.C. Dubinsky, S.R. Brant, M.S. Silverberg, R.H. Duerr, D. Altshuler, S. Gabriel, G. Lettre, A. Franke, M. D'Amato, D.P.B. McGovern, J.H. Cho, J.D. Rioux, R.J. Xavier, and M.J. Daly. 2011. Deep resequencing of GWAS loci identifies independent rare variants associated with inflammatory bowel disease. *Nature Genetics* 43:1066-1073.

Schulthess, J., S. Pandey, M. Capitani, K.C. Rue-Albrecht, I. Arnold, F. Franchini, A. Chomka, N.E. Ilott, D.G.W. Johnston, E. Pires, J. McCullagh, S.N. Sansom, C.V. Arancibia-Cárcamo, H.H. Uhlig, and F. Powrie. 2019. The Short Chain Fatty Acid Butyrate Imprints an Antimicrobial Program in Macrophages. *Immunity* 50:432-445.e437.

Segata, N., J. Izard, L. Waldron, D. Gevers, L. Miropolsky, W.S. Garrett, and C. Huttenhower. 2011. Metagenomic biomarker discovery and explanation. *Genome Biology* 12:R60.

Smythies, L.E., M. Sellers, R.H. Clements, M. Mosteller-Barnum, G. Meng, W.H. Benjamin, J.M. Orenstein, and P.D. Smith. 2005. Human intestinal macrophages display profound inflammatory anergy despite avid phagocytic and bacteriocidal activity. *115:66-75.*

Stappenbeck, T.S., and H.W. Virgin. 2016. Accounting for reciprocal host-microbiome interactions in experimental science. *Nature* 534:191-199.

Tanoue, T., S. Morita, D.R. Plichta, A.N. Skelly, W. Suda, Y. Sugiura, S. Narushima, H. Vlamakis, I. Motoo, K. Sugita, A. Shiota, K. Takeshita, K. Yasuma-Mitobe, D. Riethmacher, T. Kaisho, J.M. Norman, D. Mucida, M. Suematsu, T. Yaguchi, V. Bucci, T. Inoue, Y. Kawakami, B. Olle, B. Roberts, M. Hattori, R.J. Xavier, K. Atarashi, and K. Honda. 2019. A defined commensal consortium elicits CD8 T cells and anti-cancer immunity. *Nature* 565:600-605.

Thorsteinsdottir, U., A. Mamo, E. Kroon, L. Jerome, J. Bijl, H.J. Lawrence, K. Humphries, and G. Sauvageau. 2002. Overexpression of the myeloid leukemia-associated Hoxa9 gene in bone marrow cells induces stem cell expansion. *Blood* 99:121-129.

Vinolo, M.A.R., H.G. Rodrigues, R.T. Nachbar, and R. Curi. 2011. Regulation of Inflammation by Short Chain Fatty Acids. *Nutrients* 3:858-876.

Walujkar, S.A., D.P. Dhotre, N.P. Marathe, P.S. Lawate, R.S. Bharadwaj, and Y.S. Shouche. 2014. Characterization of bacterial community shift in human Ulcerative Colitis patients revealed by Illumina based 16S rRNA gene amplicon sequencing. *Gut Pathogens* 6:22.

Waterfield, M., I.S. Khan, J.T. Cortez, U. Fan, T. Metzger, A. Greer, K. Fasano, M. Martinez-Llordella, J.L. Pollack, D.J. Erle, M. Su, and M.S. Anderson. 2014. The transcriptional regulator Aire coopts the repressive ATF7ip-MBD1 complex for the induction of immunotolerance. *Nat Immunol* 15:258-265.

Wu, S.E., S. Hashimoto-Hill, V. Woo, E.M. Eshleman, J. Whitt, L. Engleman, R. Karns, L.A. Denson, D.B. Haslam, and T. Alenghat. 2020. Microbiota-derived metabolite promotes HDAC3 activity in the gut. *Nature* 586:108-112.

Yang, I., D. Eibach, F. Kops, B. Brenneke, S. Woltemate, J. Schulze, A. Bleich, A.D. Gruber, S. Muthupalani, J.G. Fox, C. Josenhans, and S. Suerbaum. 2013. Intestinal Microbiota Composition of Interleukin-10 Deficient C57BL/6J Mice and Susceptibility to Helicobacter hepaticus-Induced Colitis. *PLoS ONE* 8:e70783.

Yu, A.I., L. Zhao, K.A. Eaton, S. Ho, J. Chen, S. Poe, J. Becker, A. Gonzalez, D. McKinstry, M. Hasso, J. Mendoza-Castrejon, J. Whittfield, C. Koumpouras, P.D. Schloss, E.C. Martens, and G.Y. Chen. 2020. Gut Microbiota Modulate CD8 T Cell Responses to Influence Colitis-Associated Tumorigenesis. *Cell Reports* 31:107471.

Zenewicz, L.A., X. Yin, G. Wang, E. Elinav, L. Hao, L. Zhao, and R.A. Flavell. 2013. IL-22 Deficiency Alters Colonic Microbiota To Be Transmissible and Colitogenic. *The Journal of Immunology* 190:5306-5312.

Zhang, X., D. Zhao, X. Xiong, Z. He, and H. Li. 2016. Multifaceted Histone H3 Methylation and Phosphorylation Readout by the Plant Homeodomain Finger of Human Nuclear Antigen Sp100C. *Journal of Biological Chemistry* 291:12786-12798.

Zhou, L., Y. Wang, M. Zhou, Y. Zhang, P. Wang, X. Li, J. Yang, H. Wang, and Z. Ding. 2018. HOXA9 inhibits HIF-1 α -mediated glycolysis through interacting with CRIP2 to repress cutaneous squamous cell carcinoma development. *Nature Communications*. doi:10.1038/s41467-018-03914-5.

Zucchelli, C., S. Tamburri, G. Filosa, M. Ghitti, G. Quilici, A. Bachi, and G. Musco. 2019. Sp140 is a multi-SUMO-1 target and its PHD finger promotes SUMOylation of the adjacent Bromodomain. *Biochim Biophys Acta Gen Subj* 1863:456-465.